Higher Order Multipole Potentials and Electrostatic Screening Effects on Cohesive Energy and Bulk Modulus of Metallic Nanoparticles

2011 Commun. Theor. Phys. 56 1125

(http://iopscience.iop.org/0253-6102/56/6/26)

Commun. Theor. Phys. **56** (2011) 1125–1129 Vol. 56, No. 6, December 15, 2011

Higher Order Multipole Potentials and Electrostatic Screening Effects on Cohesive Energy and Bulk Modulus of Metallic Nanoparticles*

T. Barakat†

Physics Department, King Saud University, P.O. Box 2455, Riyadh 11451, Saudi Arabia

(Received May 16, 2011; revised manuscript received June 27, 2011)

Abstract *Higher order multipole potentials and electrostatic screening effects are introduced to incorporate the dangling bonds on the surface of a metallic nanopaticle and to modify the coulomb like potential energy terms, respectively. The total interaction energy function for any metallic nanoparticle is represented in terms of two- and three-body potentials. The two-body part is described by dipole-dipole interaction potential, and in the three-body part, triple-dipole (DDD) and dipole-dipole-quadrupole (DDQ) terms are included. The size-dependent cohesive energy and bulk modulus are observed to decrease with decreasing sizes, a result which is in good agreement with the experimental values of Mo and W nanoparticles.*

PACS numbers: 61.46.Df, 61.50.Lt, 78.67.Bf
Key words: higher order multipole potentials, electrostatic screening effect, size-dependent cohesive energy, size-dependent bulk modulus, metallic nanoparticles

1 Introduction

Currently, it is firmly established that when the size of materials decreases to nanoscale range, new physical and chemical properties are occurred in such systems. The most significant characteristic of materials at this scale is arising from the bond contractions of the low-coordinated atoms at the surface. Accordingly, the cohesive energy, bulk modulus, melting temperature, and other properties are observed to deviate from their bulk counterparts and became size and structure dependent properties.[1−3] Thus, to further the development of future nanoparticles applications, knowledge of the size, structure, and interatomic forces or potentials between atoms at the nanoscale is vital. Therefore, it is our interest to investigate more deeply the size-dependent cohesive energy, bulk modulus, and the structural stabilities of metallic nanoparticles.

Throughout this paper, it is assumed that a non-relaxed initial geometries of nanoparticles in nanometer sizes are constructed from a large bulk BCC or FCC crystalline structures using different spherical cutoff diameters. These nanoparticles are expected to favor densely packed structures, due to the large ratio of surface to volume atoms, creating many dangling bonds, and making a strong surface tension. Therefore, higher order multipole potentials are essential for the description of both interior and exterior atoms for these different geometries. For this reason, in this work, the total interaction energy of a nanoparticle is represented in terms of two- and three-body potentials. The two-body potential is described by a dipole-dipole interaction, and in the three-body part, triple-dipole (DDD) and dipole-dipole-quadrupole (DDQ) terms are included.[4−5]

Furthermore, each generated nanoparticle is considered like a point test charge (spherical) as it is immersed in the bulk crystal. The electron concentration near this nanoparticle will be perturbed in such a way that the electric field of the nanoparticle is cancelled by the induced disturbance of the electron concentration, thus, the nanoparticle atoms are assumed to be screened by the electron gas of the bulk crystal. Consequently, the coulomb like potential energy terms in the potential energy function are modified.[6]

Finally, the present study is based on our two recent works, where we have proposed the size-dependent potential parameters (SDPP) model to explain the cohesive energy depression of nanoparticles.[7−9]

With this in mind, this paper is structured as follows: In Sec. 2, the parametrization of the dipole-dipole interaction potential, the model and the computational method to predict the size-dependent cohesive energy and bulk modulus for Mo and W nanoparticles are discussed. In Sec. 3, the theoretical results of this work compared with the experimental ones are presented, and therein, we remark on the results and on the possible extensions of this study.

2 Model and Computational Method

In the last few years many attempts have been devoted to predict energetically the most stable structures of different nanoparticles. The *ab initio* calculations from first principles is the most familiar method. However, in spite of the advent of sophisticated computers, it is still not practical within the *ab initio* framework to handle systems containing more than a few tens of atoms,

*Supported by King Saud University, College of Science-Research Center, Project Number PHYS/2009/19
†E-mail: tbarakat@ksu.edu.sa

and it is also difficult to explore the size-dependent cohesive energy of nanoparticles using direct experimental approaches. Thus, the proper choice of a potential energy function (PEF) and a satisfactory method like SDPP is an indispensable way in nanoscience computations.[7−9]

In the SDPP model, we assume that if there is no external force acting on the nanoparticle, then a PEF $\phi_N(\overrightarrow{r_1},\ldots,\overrightarrow{r_N})$ of N atoms as function of their positions is existed, and it can be expanded quite generally into a many-body potential series containing two- and three-body potentials:[10]

$$\phi_N = \frac{1}{2!}\sum_{\substack{i\\ i\neq j}}^{N}\sum_{j}^{N} u(\overrightarrow{r_i},\overrightarrow{r_j}) + \frac{1}{3!}\sum_{\substack{i\\ i\neq j\neq k}}^{N}\sum_{j}^{N}\sum_{k}^{N} u(\overrightarrow{r_i},\overrightarrow{r_j},\overrightarrow{r_k}) + \cdots, \quad (1)$$

where $u(\overrightarrow{r_i},\overrightarrow{r_j})$ and $u(\overrightarrow{r_i},\overrightarrow{r_j},\overrightarrow{r_k})$ are the two-body and three-body potentials, respectively. This is the so-called many-body expansion of ϕ_N, ϕ_N is a measurable quantity, which describes the total configuration energy (cohesive energy) of the system, and it is usually believed that the series has a quick convergence, and therefore, the higher moments may be neglected.

The relevant two-body part in Eq. (1) is represented by the dipole-dipole interaction potential:[11]

$$u(\overrightarrow{r_i},\overrightarrow{r_j}) = \varepsilon\Big[\frac{n}{m-n}\Big(\frac{r_0}{r_{ij}}\Big)^m - \frac{m}{m-n}\Big(\frac{r_0}{r_{ij}}\Big)^n\Big], \quad r_{ij} = |r_i - r_j|, \quad (2)$$

where r_0 denotes the equilibrium separation between the centers of any two atoms, and ε is the two-body energy at $r_{ij} = r_0$. The variables m and n are the exponents for the repulsive and the attractive terms, respectively. To determine the parameters (ε, r_0, m, n) a non-linear least-squares curve fitting is performed. In the fitting procedure, we have used the binding energy values of Mo_2 and W_2 dimers calculated at various interatomic distances by *ab initio* method.[12] The potential energy curves estimated by *ab initio* method and the fitted dipole-dipole interaction potential functions for both Mo_2 and W_2 are shown in Figs. 1 and 2. The fitted dipole-dipole interaction potential parameters for Mo_2 are ($\varepsilon = 3.98$ eV, $r_0 = 1.95$ Å, $m = 8$, $n = 4$), whereas the fitted dipole-dipole interaction potential parameters for W_2 are ($\varepsilon = 4.511$ eV, $r_0 = 2.056$ Å, $m = 8$, $n = 4$). In these parameters, the energies are in electron volts and the distances are in Ångström.

Evidently, it is well known that, if the PEF of a system includes only two-body part potential, such a PEF does not stabilize open structures, and does not provide the proper atomic configuration for trimers. Therefore, the three-body terms should be included, which make important contributions to the structure including dangling bonds and the stability of different nanoparticles, is expressed as:

$$u(\overrightarrow{r_i},\overrightarrow{r_j},\overrightarrow{r_k}) = \sum_{\ell} Z_\ell G_\ell(\overrightarrow{r_i},\overrightarrow{r_j},\overrightarrow{r_k}), \quad (3)$$

where the summation includes all the triple-multipole interactions coming from the expansion of the third-order interaction energy for three atoms, and they have positive energy contribution. The parameters Z_ℓ are the interaction constants for the triple-multipole interaction terms and are to be determined.

Several multipole interactions functional forms of $G_\ell(\overrightarrow{r_i},\overrightarrow{r_j},\overrightarrow{r_k})$ have been obtained by Bell[4] and Doren and Zucker.[5] Further, it has been shown that the most important contribution is due to the triple-dipole (DDD) term, and the next dominant dipole-dipole-quadrupole (DDQ) term, which are given for closed-shell systems as:

$$G_{DDD}(\overrightarrow{r_i},\overrightarrow{r_j},\overrightarrow{r_k}) = \frac{1+3\cos\theta_i\cos\theta_j\cos\theta_k}{r_{ij}^3 r_{ik}^3 r_{jk}^3}, \quad (4)$$

$$G_{DDQ}(\overrightarrow{r_i},\overrightarrow{r_j},\overrightarrow{r_k}) = \frac{9\cos\theta_k - 25\cos 3\theta_k + 6\cos(\theta_i-\theta_j)(3+5\cos 2\theta_k)}{16\ r_{ij}^3 r_{jk}^4 r_{ki}^4}, \quad (5)$$

where θ_i, θ_j, θ_k and r_{ij}, r_{ik}, r_{jk} are the angles and the sides formed by the three particles i, j, and k, respectively.

Combining Eqs. (1) to (5) and using the fitted dipole-dipole potential parameters, the effective cohesive energy per atom ϕ_a^* for any nanoparticle with a cubic internal structure may be written as:

$$\phi_a^* = \frac{1}{2}A_8 r^{*8} - A_4 r^{*4} + Z_1^* T_{DDD} r^{*9} + Z_2^* T_{DDQ} r^{*11}, \quad (6)$$

where $\phi_a^* = \phi_N/(N\varepsilon)$, $Z_1^* = Z_1/(\varepsilon r_0^9)$, $Z_2^* = Z_2/(\varepsilon r_0^{11})$, $r^* = r_0/d$. d represents the nearest neighbor distance for any structure. A_8, A_4, T_{DDD}, and T_{DDQ} are the lattice sums and they are given by:

$$A_8 = \frac{1}{N}\sum_{\substack{i\\ i\neq j}}^{N}\sum_{j}^{N}\Big(\frac{g}{a_{ij}}\Big)^8, \quad A_4 = \frac{1}{N}\sum_{\substack{i\\ i\neq j}}^{N}\sum_{j}^{N}\Big(\frac{g}{a_{ij}}\Big)^4, \quad (7)$$

$$T_{DDD} = \frac{1}{6N}\sum_{\substack{i\\ i\neq j\neq k}}^{N}\sum_{j}^{N}\sum_{k}^{N}\frac{(1+3\cos\theta_i\cos\theta_j\cos\theta_k)}{((a_{ij}/g)(a_{ik}/g)(a_{jk}/g))^3}, \quad (8)$$

$$T_{DDQ} = \frac{1}{6N} \sum_{\substack{i \\ i\neq j\neq k}}^{N} \sum_{j}^{N} \sum_{k}^{N} \frac{(9\cos\theta_k - 25\cos 3\theta_k + 6\cos(\theta_i - \theta_j)(3 + 5\cos 2\theta_k))}{(a_{ij}/g)^3 (a_{jk}/g)^4 (a_{ki}/g)^4}, \tag{9}$$

where g is a geometrical constant that depends on the inner structure of the nanoparticle, and a_{ij} are numbers.

It is obvious that the potential parameters A_8, A_4, T_{DDD}, and T_{DDQ} are related to the particle size N, are related to the inner structure of the nanoparticle through g, and highly dependent on the potential powers. That is to say, changing the potential powers means changing the range of the potential.

On the other hand, the stability condition, which guarantees the minimum energy configurations of any nanoparticle at $T = 0^0$ K can be obtained by considering $\partial\phi_a^*/\partial V = 0$:

$$\begin{aligned} &8A_8 r^{*8} - 8A_4 r^{*4} + 18 Z_1^* T_{DDD} r^{*9} \\ &+ 22 Z_2^* T_{DDQ} r^{*11} = 0. \end{aligned} \tag{10}$$

This is because the atomic volume V is related to d through $V = N_0 g d^3$, where N_0 denotes the Avogadro's number, and r^* is related to d through $r^* = (V_0/V)^{1/3} = r_0/d$, where V_0 denotes the equilibrium volume. Thus, changing r^* means changing the volume of the nanoparticle.

Finally, the bulk modulus $B_m = V(\partial^2\phi_N/\partial V^2)$, which is related to the compressibility of a nanoparticle is given by:

$$\begin{aligned} B_m^* =& \frac{88}{18} A_8 r^{*8} - \frac{56}{18} A_4 r^{*4} + \frac{216}{18} Z_1^* T_{DDD} r^{*9} \\ &+ \frac{308}{18} Z_2^* T_{DDQ} r^{*11}, \end{aligned} \tag{11}$$

where $B_m^* = V B_m/N\varepsilon$.

By defining the first two terms of Eq. (6) as $\phi_2^*(r^*)$, the third and the last terms as $\phi_{31}^*(r^*, Z_1^*)$ and $\phi_{32}^*(r^*, Z_2^*)$, respectively. Similarly, defining the first two terms of Eq. (11) as $B_2^*(r^*)$, the third and the last terms as $B_{31}^*(r^*, Z_1^*)$ and $B_{32}^*(r^*, Z_2^*)$, respectively. Then we may express Eqs. (6) and (11) as

$$\phi_a^* = \phi_2^*(r^*) + \phi_{31}^*(r^*, Z_1^*) + \phi_{32}^*(r^*, Z_2^*), \tag{12}$$

$$B_m^* = B_2^*(r^*) + B_{31}^*(r^*, Z_1^*) + B_{32}^*(r^*, Z_2^*). \tag{13}$$

Although, the three-body terms in Eqs. (4) and (5) were derived for the closed-shell atomic systems,[4−5] the values, respectively, ϕ_a^*, r^*, and B_m^* calculated from Eqs. (6), (10), and (11) would be expected to be in good agreement with the observed values of closed-shell atomic elements. However, for other elements like Mo and W in our case, it might not be possible in the fitting procedure to reproduce the bulk observed values, because of the differences in the electronic structure. Therefore, the electrostatic screening length phenomena should be considered. So that, the screening effect $\exp(\alpha r^*)$ is assumed for r^* dependent terms, and the modified expressions of ϕ_a^* and B_m^* for any nanoparticle structure are:

$$\begin{aligned} \phi_s^* =& \exp(\alpha r^*)[\phi_2^*(r^*) \\ &+ \phi_{31}^*(r^*, Z_1^*) + \phi_{32}^*(r^*, Z_2^*)], \end{aligned} \tag{14}$$

$$\begin{aligned} B_s^* =& \exp(\alpha r^*)[B_2^*(r^*) \\ &+ B_{31}^*(r^*, Z_1^*) + B_{32}^*(r^*, Z_2^*)], \end{aligned} \tag{15}$$

where α is the screening constant. Evidently, in the fitting procedure, Eqs. (14) and (15) should now satisfy the cohesive energy and bulk modulus of bulk materials.

3 Theoretical Results, Comparison and Discussion

Calculations are carried out in unitless quantities using the reduced equations (10), (14), and (15). First, the screening constant α, and the energy parameters (Z_1^*, Z_2^*) are obtained to give the best fit to experimental data for Mo and W bulk structures. In the fitting procedure, the following values are used as input parameters for bulk Mo: $r_0 = 1.95$ Å; $\varepsilon = 3.98$ eV are taken from Fig. 1 of this work, and they are denoted as the equilibrium separation between the centers of any two atoms and the two-body energy at $r_{ij} = r_0$, respectively. $d = 2.72$ Å,[6] which is the nearest neighbor distance, $\phi_N/(N) = -6.2$ eV/atom;[6] $B_m/(N) = 230$ GPA=1.435 eV/Å^3;[13] $V = N_0 g d^3$, with $g = 0.7698$ is the geometrical factor of BCC structures. Accordingly, $r^* = r_0/d = 0.715$; $\phi_s^* = \phi_N/(N\varepsilon) = -1.557$; $B_s^* = V B_m/(N\varepsilon) = 5.58$. On the other hand, the potential parameters for bulk BCC structures are used at this stage and are taken from Refs. [14] and [5]: $A_8 = 10.360$; $A_4 = 22.640$; $T_{DDD} = 14.770$; $T_{DDQ} = 15.010$. The fitted values are $\alpha = -1.002$, $Z_1^* = 2.823$, and $Z_2^* = 0.60$. While the input parameters for bulk W are: $r_0 = 2.056$ Å; $\varepsilon = 4.511$ eV are taken from Fig. 2 of this work. $d = 2.73$ Å;[6] $\phi_N/(N) = -8.55$ eV/atom;[6] $B_m/(N) = 310$ GPA=1.934 eV/Å^3.[13] Accordingly, $r^* = r_0/d = 0.753$; $\phi_s^* = \phi_N/(N\varepsilon) = -1.895$; $B_s^* = V B_m/(N\varepsilon) = 6.70$, and the fitted values are $\alpha = -1.052$, $Z_1^* = 2.036$, and $Z_2^* = 0.60$.

Consequently, in the nano-range, the potential parameters A_8, A_4, T_{DDD}, and T_{DDQ} are all depended on the particle size through N, and the investigation is carried out for BCC and FCC nanoparticles using various spherical diameters $1 \leq R_{\rm cut} \leq 10$. For each value of $R_{\rm cut}$ a new nanoparticle with new size is generated. The variations of A_8, A_4, and T_{DDD} with the particle size and with different structures were calculated in [8], whereas, in this work the variation of T_{DDQ} with the particle size and with different structures are obtained.

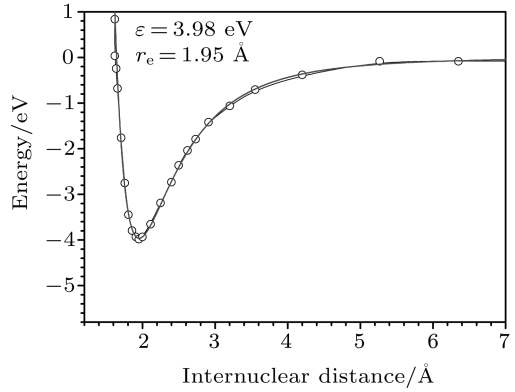

Fig. 1 Potential energy curve of the Mo_2 dimer. Circles are *ab initio*;[12] solid line is the fitted dipole-dipole potential.

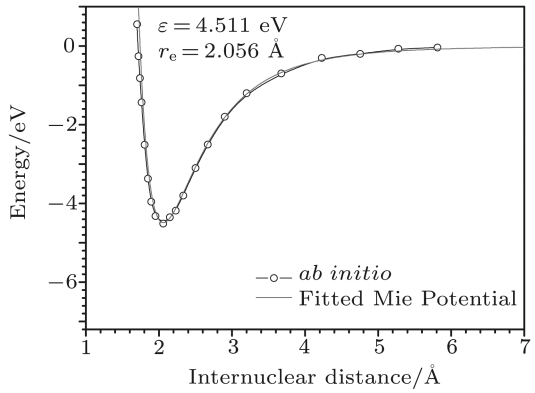

Fig. 2 Potential energy curve of the W_2 dimer. Circles are *ab initio*;[12] solid line is the fitted dipole-dipole potential.

For every generated Mo nanoparticle of inner structure BCC or FCC, r^*'s are calculated from the stability condition at $Z_1^* = 2.823$ and $Z_2^* = 0.6$, whereas, for W nanoparticles, r^*'s are calculated from the stability condition at $Z_1^* = 2.036$ and $Z_2^* = 0.6$, respectively. The positive real root of Eq. (10) is assumed as an acceptable solution. Then ϕ_s^* and B_s^* for Mo nanoparticles with different structures are calculated as a function of N at $\alpha = -1.052$, whereas, ϕ_s^* and B_s^* for W nanoparticles with different structures are calculated as a function of N at $\alpha = -1.002$.

Typically, to make the size-dependent cohesive energy free from the parameter ε, we calculate the relative cohesive energy of any nanoparticle with respect to the cohesive energy of the corresponding bulk material i.e. ϕ_s^*/ϕ_0^*, where we denotes the relative cohesive energy of bulk material by ϕ_0^*. It is reported that the cohesive energy of Mo nano-particle in the size $N = 2000$ is -4.25 eV/atom,[15] whereas the cohesive energy of bulk Mo is -6.2 eV/atom.[6] On the other hand, for the W nano-particle in the size $N = 7000$, it's cohesive energy is -6.42 eV/atom,[15] and that of the corresponding bulk W is -8.55 eV/atom.[6]

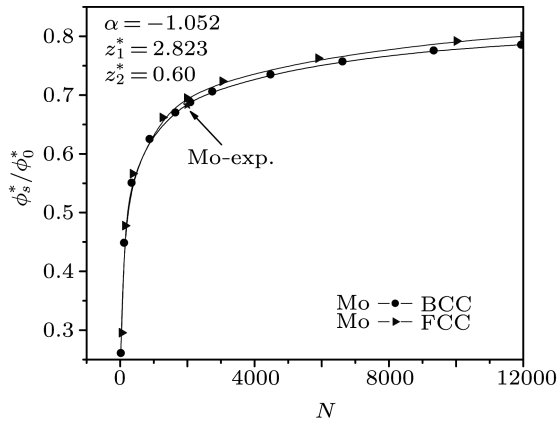

Fig. 3 The particle size dependence of the relative cohesive energy of BCC and FCC Mo nanoparticles. The star symbols denote the experimental values.[15]

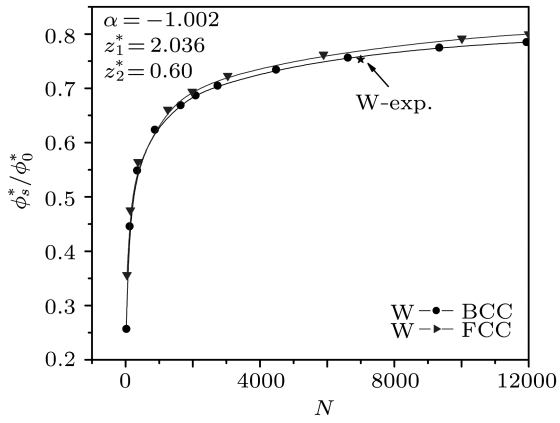

Fig. 4 The particle size dependence of the relative cohesive energy of BCC and FCC W nanoparticles. The star symbols denote the experimental values.[15]

The results of SDPP model for the relative cohesive energy and the bulk modulus of Mo and W nanoparticles with different sizes and different structures are shown in Figs. 3–6. In these figures the solid-symbol lines are the results calculated by Eqs. (14) and (15), and those with the star symbols are denoted the experimental values of Mo and W nanoparticles.[15]

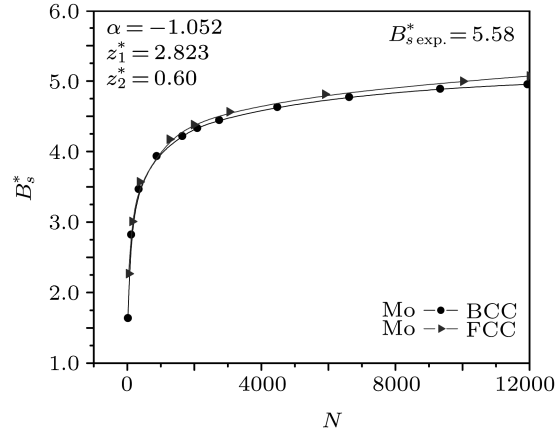

Fig. 5 The particle size dependence of the bulk modulus of BCC and FCC Mo nanoparticles.

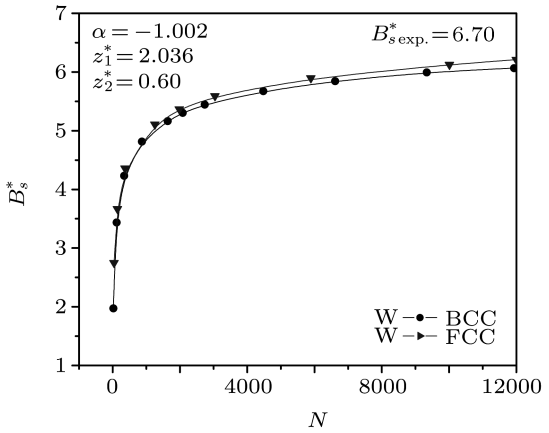

Fig. 6 The particle size dependence of the bulk modulus of BCC and FCC W nanoparticles.

From figures, the relative cohesive energy and the bulk modulus of nanoparticles increase when the particle size is increased, and approaches to that of the corresponding bulk metal when N is very large, which reflects the instability of wholly free-standing nanoparticle in comparison with the corresponding bulk metal. However, for wholly embedded nanopartile in a matrix, the situation may be different and we will discuss this case in a separate work. Generally speaking, it was shown that the cohesive energy of a nanoparticle can be increased or decreased depending on the degree of coherence between the nanoparticle and the matrix.[16−17]

Also, we noted from Figs. 3 and 4 that the more densely packed structures are favored in the range $15 < N < 2000$ atoms, which means that nanoparticles undergo structural phase transitions from BCC to FCC. Evidently, to understand the phase transitions the minimum cohesive energy per atom versus randomly atomic volume $r^* = (V_0/V)^{1/3}$ for W nanoparticle of size ≈ 140 atoms in BCC and FCC crystalline structures are show in Fig. 7. From this figure we note that, the more densely packed structure FCC is favored at $r^* = 0.7$ which is in this model the real equilibrium atomic volume of the W nanoparticle of size ≈ 140 atoms, supporting the idea that nanoparticles usually tend to decrease their surface area in order to lower the surface energy.[18]

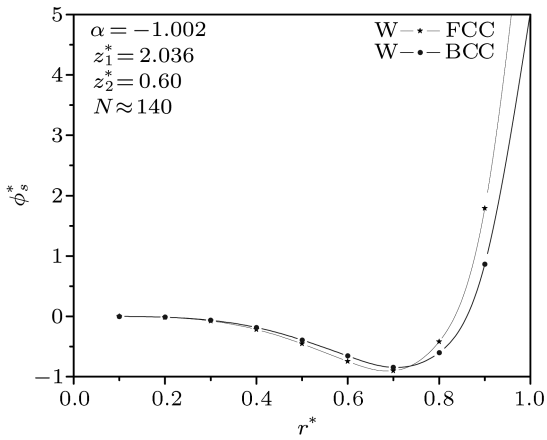

Fig. 7 Variation of cohesive energy per atom versus atomic volume r^* for W nanoparticle of size ≈ 140 atoms in BCC and FCC structures.

In conclusion, the results obtained in this study are regarded as additional evidence that the screening effects and the multi-body forces are important to explain the structural properties of nanoparticles. Also, the predicted results are consistent with the corresponding experimental values for the cohesive energy of Mo and W nanoparticles, and suggest that the two-body dipole-dipole potential plus three body-potential including the triple-dipole and dipole-dipole-quadrupole terms can be a possible candidate to study the properties of various metallic nanoparticles by considering the size-dependent potential parameters model.

References

[1] K.K. Nanda, S.N. Sahu, and S.N. Behera, Phys. Rev. A **66** (2002) 13208.

[2] W.H. Qi, M.P. Wang, and G.Y. Xu, Chem. Phys. Lett. **372** (2003) 632.

[3] W.H. Qi and M.P. Wang, Mater. Chem. Phys. **88** (2004) 280.

[4] R.J. Bell, J. Phys. B **3** (1970) 751.

[5] M.B. Doran and I.J. Zucker, J. Phys. C **4** (1971) 307.

[6] C. Kittel, *Introduction to Solid State Physics*, 7th ed, Wiley, New York (1996).

[7] T. Barakat, O.M. Al-Dossary, and A.A. Alharbi, Int. J. Nanosci. **6** (2007) 461.

[8] T. Barakat, O.M. Al-Dossary, and E.H. Abdul-Hafidh, J. Phys. B **42** (2009) 165104.

[9] E.H. Abdul-Hafidh, T. Barakat, and O.M. Al-Dossary, J. Comput. Theor. Nanosci. **8** (2011) 1134.

[10] T. Halicioğlu, Phys. Stat. Sol. (b) **99** (1980) 347.

[11] G. Mie, Ann. Phys. Leipzig **11** (1903) 657.

[12] C. Angli, A. Cavallini, and R. Cimiraglia, J. Chem. Phys. **127** (2007) 074306.

[13] www.webelemets.com, *WebElements: the Periodic Table on the Web*.

[14] N.W. Ashcroft and N.D. Mermin, *Solid State Physics, Holt-Saunders International Edition*, Holt, Rinehart and Winston, New York (1976).

[15] H.K. Kim, S.H. Huh, J.W. Park, J.W. Jeong, and G.H. Lee, Chem. Phys. Lett. **354** (2002) 165.

[16] W.H. Qi, M.P. Wang, M. Zhou, and W.Y. Hu, J. Phys. D **38** (2005) 1429.

[17] D. Xie, M.P. Wang, and W.H. Qi, J. Phys. Condens. Matter **16** (2004) L401.

[18] Q. Jiang, J.C. Li, and B.Q. Chi, Chem. Phys. Lett. **366** (2002) 551.